Int. J. Solids Structures, Vol. 18, No. 1, pp. 37–49, 1982
Printed in Great Britain.

0020-7683/82/010037–13$03.00/0

AN EFFICIENT FINITE ELEMENT SCHEME FOR ELASTIC POROUS MEDIA

WORSAK KANOK-NUKULCHAL and VIDANERALALAGE WIMAL SUARIS
Division of Structural Engineering and Construction, Asian Institute of Technology, P.O. Box 2754, Bangkok, Thailand

(*Received* 3 *December* 1980)

Abstract—A semi-analytical finite element scheme for the analysis of diffusion process in linear elastic porous media is presented. Variational principle based on Biot's Theory serves to establish discretized equilibrium and flow equations in terms of nodal displacements and fluid pore pressures. Time dependency of the system is removed by the Laplace transformation.

The Laplace transforms of nodal pore pressures can be obtained by solving a standard eigenvalue system after releasing all nodal displacements through condensation. In the case of step loads commonly found in consolidation problems, the Laplace transforms can be inverted analytically. For general loading however, a series of step loads is introduced as its approximation, and the final solution is obtained by superposiiton.

Three types of quadrilateral plane-strain finite elements are tested for their performance in solving 2-D consolidation problems by the present scheme. The quadrilateral element with eight displacement and four pore pressure nodes shows the best overall performance. Results from numerical examples indicate that the present scheme is extremely efficient. Solution of both the pore pressure and the displacement fields at any specified time can be determined explicitly without intermediate solutions.

INTRODUCTION

A broad class of physical phenomena can be described by the diffusion process in linear elastic porous media. Obvious examples are problems of consolidation and seepage. Interest in the behaviour of porous media can be traced back to the work of Terzaghi[1] in which a theory of one dimensional consolidation was presented. Many contributions have since been made for various improvements[2]. A theory of three dimensional consolidation was presented by Biot[3]. Biot's equations are complicated by the coupling between the elasticity problem and the diffusion process; consequently, closed form solutions are available only to simple problems with regard to geometry, loading and boundary conditions[4]. Because of this shortcoming, attempts have been made to apply numerical techniques to this class of problems.

A finite element scheme was first proposed by Sandhu[5] for the analysis of seepage in elastic media. This finite element solution was based on a variational principle in which displacement and fluid pore pressure are primary field variables. Subsequent researchers[6–8] attempted to improve the solution in many aspects. Yokoo *et al.*[9] presented a more general variational principle which admits interelement discontinuities of the field variables. Recently, Krauss[10] proposed a finite element scheme based on the virtual work principle. The principle of virtual displacement is used to establish a set of generalized equilibrium equations for the medium, while the Lagrange multiplier technique enforces the interelement continuity conditions.

For spatial discritization, many researchers[5, 6, 8] employed triangular elements. Valliappan *et al.*[7] used an eight-node isoparametric quadrilateral element. Recently Sandhu *et al.*[11] compared the performances of several finite elements: defficiencies were reported in the elements using the same set of interpolation functions for both the pore pressure and displacement fields.

In conjunction with the spatial discretization, time integration methods are often used for temporal discretization. In general, time integration technique entails very small time step for solutions at the earlier stage of the diffusion process. If solutions are required after a long duration the size of time step may be increased several times for economic reason. Each time step change however requires a new matrix factorization, and thus increases the computational cost.

In this study, a semi-analytical finite element scheme is proposed. Based on Biot's theory, spatial discretization of linear elastic porous media is conducted through a finite element idealization. The Laplace transformation serves to remove its time dependency.

Three quadrilateral plane-strain elements with varying interpolation orders of displacement and the pore pressure fields are tested, in the attempt to determine the best performing element under the present scheme.

FORMULATION

Analysis of the Newtonian fluid diffusion process in a saturated, linear elastic porous medium by Biot's theory[3] employs the following assumptions.

(1) The elastic medium is isotropic and saturated with incompressible fluid.
(2) Deformation of the elastic medium depends on the effective stresses.
(3) Fluid flow through the elastic medium is governed by Darcy's law.
(4) Deformations and velocities are small.

Field equations

Figure 1 shows a region R occupied by the elastic medium of which the volume is denoted by V and the boundary surface by S. Boundary conditions associated with the elastic deformation consist of a prescribed surface traction $\hat{T}$ on S_T and a prescribed displacement $\hat{U}$ on S_U, where $S_T + S_U = S$. On the same surface, boundary conditions associated with the fluid diffusion process are the prescribed pore pressure $\hat{P}$ on S_P and the prescribed normal outflow of fluid, $\hat{Q}$, across S_Q, where $S_P + S_Q = S$.

The governing equations for the combined elasticity problem and diffusion process are given as follows[3].

(a) Equilibrium equations:

$$\sigma_{ij,j} + \delta_{ij} p_{,j} + \rho F_i = 0 \tag{1}$$

where σ, p, ρ, F are, respectively, the effective stress tensor, the excess pore pressure of fluid, the mass density of the medium and the body force vector. The symbol δ_{ij} denotes the Kronecker delta. Subscripts after a comma denote spatial differentiation in the standard indicial notation and repeated indices imply summation.

(b) Stress–strain relationship:

$$\sigma_{ij} = E_{ijkl} \epsilon_{kl} \tag{2}$$

where $\mathbf{E}$ denotes the fourth-order elasticity tensor of the medium and ϵ is the infinitesimal

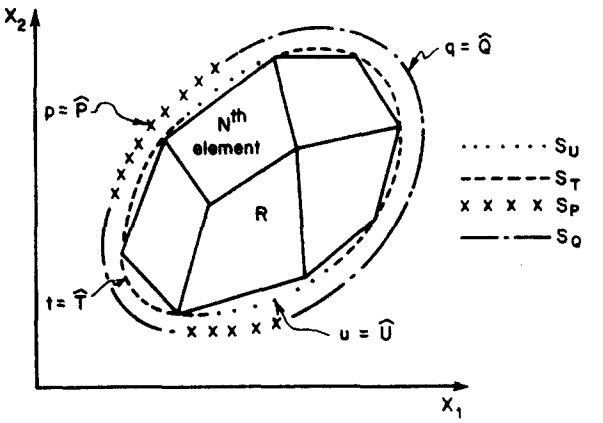

Fig. 1. Finite element idealization of a 2-D porous medium.

strain tensor given by,

$$\epsilon_{ij} = \tfrac{1}{2}(u_{i,j} + u_{j,i}) \tag{3}$$

in which $\mathbf{u}$ is the displacement vector.

(c) Equations of continuity:

The condition of saturation implies that

$$\dot{\epsilon}_{ii} = -v_{i,i} \tag{4}$$

where v is the fluid velocity vector relative to the medium and $(\cdot) = \mathrm{d}(\cdot)/\mathrm{d}t$. The fluid velocity is governed by the generalized Darcy's law such that

$$v_i = -H_{ij}(p_{,j} + \rho_f F_j) \tag{5}$$

where $\mathbf{H}$ is the permeability tensor and ρ_f the mass density of the pore fluid.

Assuming no instantaneous volume change at the initial state ($t = 0$) when the load is applied, the convolution product associated with eqn (4) at any time t, in view of eqns (3) and (5), can be written as,

$$g * \{H_{ij}(p_{,j} + \rho_f F_j)\}_{,i} + u_{i,i} = 0 \tag{6}$$

where $g = 1$. The convolution product is defined as

$$A(x,t) * B(x,t) = \int_0^t A(x, t-\tau)B(x,\tau)\,\mathrm{d}\tau. \tag{7}$$

(d) Boundary conditions:

Traction and displacement boundary conditions associated with a deformation of elastic medium are

$$n_i(\sigma_{ij} + \delta_{ij}P) = \hat{T}_j \quad \text{on } S_T \tag{8}$$

$$u_i = \hat{U}_i \quad \text{on } S_U. \tag{9}$$

For diffusion process, boundary conditions associated with the flow of pore fluid are the prescribed pore pressure,

$$p = \hat{P} \quad \text{on } S_p \tag{10}$$

and the prescribed outflow of the pore fluid

$$n_i v_i = \hat{Q} \quad \text{on } S_Q \tag{11}$$

where n_i is the outward unit normal vector to the boundary surface of R.

Variational principle

A functional $\pi(\mathbf{u}, p)$ can be constructed in terms of $\mathbf{u}$ and p which are taken as primary field variables subject to eqns (2), (3), (9) and (10). The trial functions of $\mathbf{u}$ and p that produce stationary value of π will automatically satisfy the field equations, eqns (1) and (6), and the

natural boundary conditions, eqns (8) and (11), at any time $t \in [0, \infty)$. An expression of π can be written as[5].

$$\pi(\mathbf{u}, p) = \int_R \left[\frac{1}{2}\sigma_{ij} * u_{(i,j)} - \rho F_i * u_i + p * u_{i,i} - \frac{1}{2} g * v_i * (p_{,i} + \rho_f F_i)\right] dv$$
$$- \int_{S_T} [\hat{T}_i * u_i]\, ds + \int_{S_Q} [g * \hat{Q} * p]\, ds \tag{12}$$

in which $u_{i,j} \equiv \frac{1}{2}(u_{i,j} + u_{j,i})$.

Finite element discretization

The region R is discretized into an assemblage of quadrilateral finite elements as shown in Fig. 1. In view of eqn (12), only the displacement and the pressure fields are required to be continuous over the domain. As a result, eqn (12) can be written as the accumulation of individual element contributions, i.e.

$$\pi(\mathbf{u}, p) = \sum_e \pi^e(\mathbf{u}, p) \tag{13}$$

in which

$$\pi^e(\mathbf{u}, p) = \int_{R^e} \left[\frac{1}{2}\sigma_{ij} * u_{(i,j)} - \rho F_i * u_i + p * u_{i,i} - \frac{1}{2} g * v_i * (p_{,i} + \rho_f F_i)\right] dv$$
$$- \int_{S_T^e} [\hat{T}_i * u_i]\, ds + \int_{S_Q^e} [g * \hat{Q} * p]\, ds \tag{14}$$

where R^e denotes the element domain and S_T^e and S_Q^e are respectively parts of S_T and S_Q that are associated with the element.

The displacement field $\mathbf{u}$ and the fluid pore pressure field p within each element can be expressed in terms of their nodal values by using the shape functions N_u and N_p respectively, i.e.

$$\mathbf{u}(\mathbf{x}, t) = \sum_{I=1}^{n_u} N_u^I(\mathbf{x})\mathbf{U}^I(t) \tag{15}$$

$$p(\mathbf{x}, t) = \sum_{I=1}^{n_p} N_p^I(\mathbf{x})p^I(t) \tag{16}$$

where $\mathbf{U}^I(t)$ and $P^I(t)$ are, respectively, the displacement vector and the pore pressure at node I and n_u, n_p are numbers of element nodes associated with $\mathbf{u}$ and p respectively. This element will be referred to as $Q_{n_u n_p}$. Three such quadrilateral elements Q84, Q88 and Q94 are shown in Fig. 2.

Substituting the trial displacement field, eqn (15), into eqn (3) leads to

$$\boldsymbol{\epsilon}(\mathbf{x}) = \sum_{I=1}^{n_u} \mathbf{B}_u^I(\mathbf{x})\mathbf{U}^I(t) \tag{17}$$

$$\Delta V(\mathbf{x}) = \sum_{I=1}^{n_u} \mathbf{B}_\Delta^I(\mathbf{x})\mathbf{U}^I(t) \tag{18}$$

where for plane strain problem $\boldsymbol{\epsilon} \equiv \langle \epsilon_{11}\ \epsilon_{22}\ 2\epsilon_{21} \rangle^T$, $\Delta V \equiv u_{k,k}$,

$$\mathbf{B}_u^I = \begin{bmatrix} N_{u,1}^I & 0 \\ 0 & N_{u,2}^I \\ N_{u,2}^I & N_{u,1}^I \end{bmatrix} \tag{19}$$

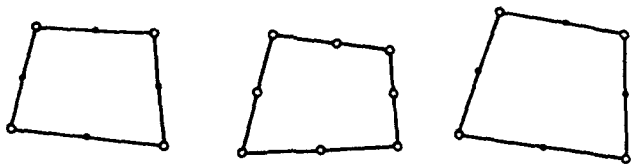

(a) ELEMENT Q84 (b) ELEMENT Q 88 (c) ELEMENT Q94

o BOTH DISPLACEMENT AND PRESSURE D.O.F
• DISPLACEMENT D.O.F ONLY

Fig. 2. Three quadrilateral plane strain elements proposed for two-dimensional linear elastic porous media.

and

$$\mathbf{B}_{\Delta}{}^{I} = [N^{I}_{u,1} \quad N^{I}_{u,2}]. \tag{20}$$

Similarly, the pore pressure gradient vector $\Delta \mathbf{p} = \langle P_{,1}\, P_{,2}\rangle^{T}$ can be obtained in terms of nodal pore pressures from eqn (16) as

$$\Delta \mathbf{p} = \sum_{I=1}^{n_p} \mathbf{B}_p{}^{I}(\mathbf{x})\mathbf{p}^{I}(t) \tag{21}$$

where

$$\mathbf{B}_p{}^{I} = \begin{bmatrix} N^{I}_{p,1} \\ N^{I}_{p,2} \end{bmatrix}. \tag{22}$$

The effective stress vector $\boldsymbol{\sigma} \equiv \langle \sigma_{11}\, \sigma_{22}\, \sigma_{21}\rangle^{T}$ in view of eqn (2) can be expressed in terms of nodal displacements as

$$\boldsymbol{\sigma} = \sum_{I=1}^{n_u} \mathbf{D}\mathbf{B}_u{}^{I}(\mathbf{x})\mathbf{U}^{I}(t) + \boldsymbol{\sigma}_0 \tag{23}$$

in which the elasticity matrix $\mathbf{D}$ is defined by $\boldsymbol{\sigma} = \mathbf{D}\boldsymbol{\epsilon} + \boldsymbol{\sigma}_0$ where, $\boldsymbol{\sigma}_0$ is the corresponding initial stress tensor.

Substituting eqns (15)–(23) into eqn (14) yields

$$\begin{aligned}\pi^{e}(\mathbf{U},\mathbf{P}) = {} & \sum_{I=1}^{n_u}\sum_{J=1}^{n_u} \frac{1}{2}[\mathbf{U}^{I}(t)]^{T} * k^{IJ}\mathbf{U}^{J}(t) - \sum_{I=1}^{n_u}[\mathbf{U}^{I}(t)]^{T} * \mathbf{b}_1{}^{I} \\ & + \sum_{I=1}^{n_u}[\mathbf{U}^{I}(t)]^{T} * \mathbf{b}_2{}^{I} + \sum_{I=1}^{n_u}\sum_{J=1}^{n_p}[\mathbf{U}^{I}(t)]^{T} * c^{IJ}P^{J}(t) \\ & - \sum_{I=1}^{n_p}\sum_{J=1}^{n_p}\frac{1}{2}P^{I}(t) * m^{IJ} * P^{J}(t) - \sum_{J=1}^{n_p} g * P^{I}(t) * b_3{}^{I} \\ & - \sum_{J=1}^{n_u}[\mathbf{U}^{I}(t)]^{T} * \mathbf{r}_1{}^{I} + \sum_{I=1}^{n_p} g * P^{I}(t) * r_2{}^{I}\end{aligned} \tag{24}$$

in which

$$\mathbf{k}^{IJ} = \int_{R^e} [\mathbf{B}_u{}^{I}]^{T}\mathbf{D}\mathbf{B}_u{}^{J}\, dv \tag{25}$$

$$m^{IJ} = \int_{R^e} [\mathbf{B}_p{}^{I}]^{T}\mathbf{H}\mathbf{B}_p{}^{J}\, dv \tag{26}$$

$$\mathbf{c}^{IJ} = \int_{R^e} [\mathbf{B}_\Delta{}^I]^T N_u{}^J \, dv \tag{27}$$

$$\mathbf{b}_1{}^I = \int_{R^e} \rho N_u{}^I \mathbf{F} \, dv \tag{28}$$

$$\mathbf{b}_2{}^I = \int_{R^e} [\mathbf{B}_u{}^I]^T \boldsymbol{\sigma}_0 \, dv \tag{29}$$

$$b_3{}^I = \int_{R^e} \rho_f [\mathbf{B}_p{}^I]^T \mathbf{H} \mathbf{F} \, dv \tag{30}$$

$$\mathbf{r}_1{}^I = \int_{S_T{}^e} N_u{}^I \hat{\mathbf{T}} \, ds \tag{31}$$

$$r_2{}^I = \int_{S_Q{}^e} N_p{}^I \hat{Q} \, ds. \tag{32}$$

Substituting eqn (24) into eqn (13) and equating the first variation of π to zero lead to a discretized governing system in the form:

$$\begin{bmatrix} \mathbf{K} & \mathbf{C} \\ \mathbf{C}^T & -g * \mathbf{M} \end{bmatrix} \begin{Bmatrix} \mathbf{U}(t) \\ \mathbf{P}(t) \end{Bmatrix} = \begin{Bmatrix} \mathbf{B}_1 - \mathbf{B}_2 + \mathbf{R}_1 \\ g * \mathbf{B}_3 - g * \mathbf{R}_2 \end{Bmatrix} \tag{33}$$

in which

$$\mathbf{U} = \langle \mathbf{U}^1 \mathbf{U}^2, \ldots\ldots\ldots\ldots \mathbf{U}^{m_u} \rangle^T \tag{34}$$

$$\mathbf{P} = \langle P^1 P^2, \ldots\ldots\ldots\ldots P^{m_p} \rangle^T \tag{35}$$

where m_u and m_p are respectively total numbers of non-prescribed displacement nodes and pore pressure nodes. The notations $\mathbf{K}$, $\mathbf{C}$, $\mathbf{M}$, $\mathbf{B}_1$, $\mathbf{B}_2$, $\mathbf{B}_3$, $\mathbf{R}_1$ and $\mathbf{R}_2$ indicate the matrices resulted from assembling individual element contributions of $\mathbf{k}$, $\mathbf{c}$, m, $\mathbf{b}_1$, $\mathbf{b}_2$, b_3, $\mathbf{r}_1$ and r_2 respectively.

The first of eqn (33) is the discretized equilibrium equation in which $\mathbf{K}$ is the usual elastic stiffness of the medium; $\mathbf{C}$ denotes the coupling effect of a unit nodal pore pressure; $\mathbf{B}_1$ is the load vector due to the body forces; $\mathbf{B}_2$ is the load vector due to initial stresses existing in the medium before the application of external load and $\mathbf{R}_1$ is the load vector due to boundary tractions. The second equation represents the discretized flow equation which relates volumetric strain to the inflow due to the nodal pore pressures, the fluid gravitational force $\mathbf{B}_3$ and the specified boundary flow $\mathbf{R}_2$.

Laplace transformation of temporal variables

Laplace transform is used to remove the time dependence and replace it by an algebraic dependence on the transform parameter. The Laplace transform of eqn (33) is given by

$$\begin{bmatrix} \mathbf{K} & \mathbf{C} \\ \mathbf{C}^T & -\frac{1}{s}\mathbf{M} \end{bmatrix} \begin{Bmatrix} \bar{\mathbf{U}} \\ \bar{\mathbf{P}} \end{Bmatrix} = \begin{Bmatrix} \bar{\mathbf{B}}_1 - \bar{\mathbf{B}}_2 + \bar{\mathbf{R}}_1 \\ \frac{1}{s}\bar{\mathbf{B}}_3 - \frac{1}{s}\bar{\mathbf{R}}_2 \end{Bmatrix} \tag{36}$$

in which s is the Laplace transform parameter and a bar denotes the Laplace transform, e.g.

$$\bar{x} = \int_0^\infty x(t) \, e^{-st} \, dt. \tag{37}$$

Equation (36) can be rearranged as

$$\begin{bmatrix} \mathbf{0} & \mathbf{0} \\ \mathbf{0} & \mathbf{M} \end{bmatrix} \begin{Bmatrix} \bar{\mathbf{U}} \\ \bar{\mathbf{P}} \end{Bmatrix} - s \begin{bmatrix} \mathbf{K} & \mathbf{C} \\ \mathbf{C}^T & \mathbf{0} \end{bmatrix} \begin{Bmatrix} \bar{\mathbf{U}} \\ \bar{\mathbf{P}} \end{Bmatrix} = \begin{Bmatrix} -s\bar{\mathbf{B}}_1 + s\bar{\mathbf{B}}_2 - s\bar{\mathbf{R}}_1 \\ -\bar{\mathbf{B}}_3 + \bar{\mathbf{R}}_2 \end{Bmatrix} \tag{38}$$

which is then condensed by eliminating $\bar{U}$, to have

$$(\mathbf{M}+s\mathbf{L})\bar{\mathbf{P}}=s\bar{\mathbf{F}} \tag{39}$$

where

$$\mathbf{L}=\mathbf{C}^T\mathbf{K}^{-1}\mathbf{C} \tag{40}$$

$$\bar{\mathbf{F}}=\left\{-\frac{1}{s}\bar{\mathbf{B}}_3+\frac{1}{s}\bar{\mathbf{R}}_2+\mathbf{C}^T\mathbf{K}^{-1}(\bar{\mathbf{B}}_1-\bar{\mathbf{B}}_2+\bar{\mathbf{R}}_1)\right\}. \tag{41}$$

Equation (39) constitutes a classical eigenvalue problem for which the solution is given in the form[12]

$$\bar{P}=\sum_{i=1}^{m_p}\frac{s}{s-s_i}\bar{a}_i\mathbf{Q}_i \tag{42}$$

in which s_i, $i=1,\ldots\ldots m_p$ are the eigenvalues of eqn (39), $\mathbf{Q}_i$ is the eigenvector associated with s_i and,

$$\bar{a}=\mathbf{Q}_i^T\bar{\mathbf{F}}/(\mathbf{Q}_i^T\mathbf{L}\mathbf{Q}_i). \tag{43}$$

The Laplace transform inversion[13] of eqn (42) leads to the solution of $\mathbf{P}(t)$ in the form

$$\mathbf{P}(t)=\sum_{i=1}^{m_p}\mathbf{Q}_i\left\{a_i(0)\,e^{s_it}+\int_0^t\frac{da_i(\tau)}{d\tau}e^{s_i(t-\tau)}\,d\tau\right\}. \tag{44}$$

For a case of step loading applied at time $t=0$, $\mathbf{P}(t)$ can be reduced to

$$\mathbf{P}(t)=\sum_{i=1}^{m_p}\mathbf{Q}_i\{a_i(0)\,e^{s_it}\}. \tag{45}$$

For simple load history cases, we still can evaluate $P(t)$ directly from eqn (44). For more complicated cases, however, the load history can be approximated by a series of step loads and its solution can be obtained via superposition.

NUMERICAL RESULTS AND DISCUSSIONS

Several examples are used to illustrate the efficiency of the present scheme. The results are compared with available solutions regarding accuracy and computational effort.

One dimensional consolidation problem Figure 3 shows two finite element models for a linear elastic soil column. One dimensional consolidation of this soil column under a constant surface loading is analysed. In this study three types of quadrilateral elements, namely, Q84, Q88 and Q94 (Fig. 2) are tested for their performances. A 2×2 G quadrature is employed uniformly for all the three elements.

These three finite elements are used to medel a linear elastic soil column as shown in Fig. 3(a); results of the surface displacement are compared in Table 1. Analytical solution[14] based on Terzaghi's one dimensional theory of consolidation and the solution by Sandhu's scheme[11] are also tabulated. Both Q84 and Q94 elements employing the 2×2 quadrature yield practically identical results, which are in good agreement with Sandhu's and the analytical solutions. The Q88 element with 2×2 quadrature gives very poor results; better performance however is obtained by increasing the order of quadrature in this case to a 3×3. Similar increase of the quadrature order is found to give no improvement on the solutions obtained by Q84 and Q94 elements.

Table 1. One dimensional consolidation problem. Comparison of the surface settlements obtained by different schemes

Time Factor $T_v = C_v t/H^2$ \ Element Type	Present Scheme			Sandhu's Temporal Discretization Scheme [11]		Analytical Solution by Scott [14]
	Q84	Q88*	Q94	Q84	Q88	
0.0	0.008247	-	0.008237	-	-	0.0
0.000021	0.009474	0.005170	0.009462	0.009173	0.004583	0.0051699
0.000042	0.010615	0.007310	0.010604	0.010335	0.006880	0.0073111
0.000105	0.013637	0.011561	0.013626	0.013403	0.011281	0.0115600
0.000630	0.029096	0.028332	0.029078	0.028995	0.028205	0.0283162
0.001154	0.038905	0.038336	0.038905	0.038832	0.038274	0.0383404
0.022146	0.169270	0.167200	0.169270	0.167780	0.166276	0.1671920
0.043137	0.235856	0.234386	0.235856	0.235313	0.233820	0.2343582
0.064128	0.287472	0.285820	0.287472	0.287183	0.285541	0.2857453
0.106111	0.369581	0.367560	0.369581	0.369520	0.367538	0.3675682
0.316023	0.631705	0.628214	0.631705	0.632652	0.629232	0.6285880
0.525936	0.782513	0.778655	0.782329	0.783582	0.779762	0.7785834
1.155674	0.955180	0.953340	0.955180	0.955670	0.953776	0.9531839
5.353924	0.999918	0.999999	0.999918	0.999900	0.999896	0.9999984

* A 3 × 3 Gaussion quadrature is employed for this case; otherwise, 2 × 2 Gaussion quadrature is used. Element Q88 using 2 × 2 Gaussian quadrature gives very poor solutions, which are not shown here.

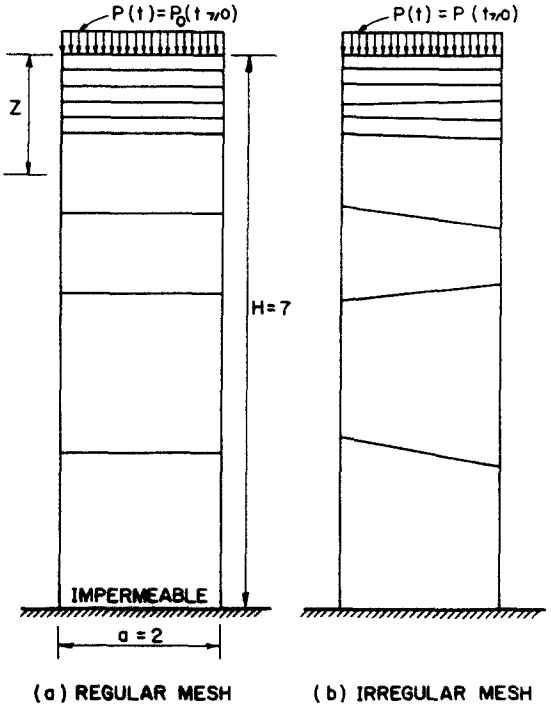

Fig. 3. Two finite element meshes for one dimensional consolidation of a soil column, of which Young's modulus $E = 6000$, Poisson's ratio $\nu = 0.4$, $k = 4 \times 10^{-6}$ and $c_v = 0.05143$.

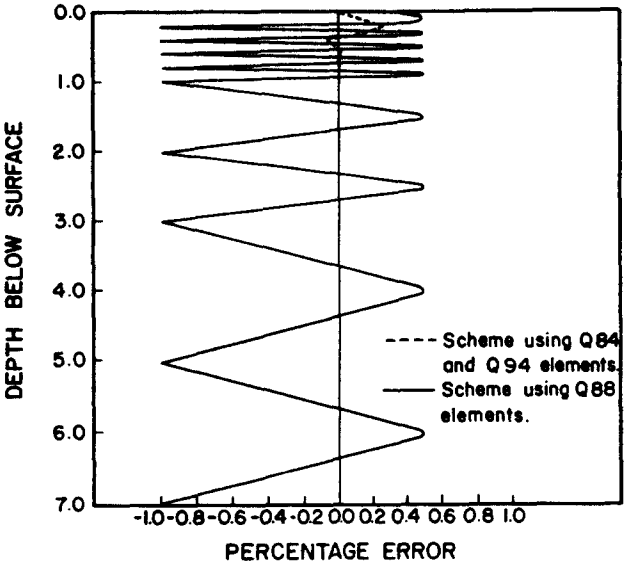

Fig. 4. Soil column consolidation problem; errors in pore pressure profile at time=0.0, using Q84, Q94 and Q88 elements.

Error in the pore pressure distribution is plotted in Fig. 4. The result points to the disadvantage of the Q88 element as it gives spurious solution for the initial pore pressure along the depth of the soil column.

The computer times required to solve this problem are recorded. The IBM 370/145 at the Asian Institute of Technology Regional Computer Center, was used and the CPU times of 31.60, 217.79 and 32.25 sec were reported for the models using Q84, Q88 and Q94 elements respectively.

The main computational effort of the present scheme is due to the eigenvalue solution of eqn (39). Thereafter, the pore pressure solution at any time can be obtained directly from the closed form expression (eqn (44)) with relatively small effort. Since the size of the eigenvalue system is controlled by the total number of pore pressure degrees of freedom, it is advantageous to keep these degrees of freedom at minimum. This also explains the considerable amount of computer time spent for the Q88 solution. The case of Q88 element which employs 8 pressure nodes needs about 6–7 times as much computer time as required by the Q84 and Q94 elements, both employing 4 pressure nodes. For this reason coupled with its poor performance in representing the pore pressure field, the Q88 element will not be considered any further in this study.

To further investigate the performance of the Q84 and Q94 elements, an irregular mesh shown in Fig. 3(b) is tested. The surface settlements at the mid point of the soil column obtained with these two elements are shown in Table 2. No significant difference can be concluded in comparing the two solutions. The Q84 element will be employed however in the following examples simply because of its smaller computational effort.

The excess pore pressure history at depths $Z/H = 2/70$ and $Z/H = 4/70$ are shown in Figs. 5(a) and 5(b) respectively. The solution by Sandhu's scheme[11] and the analytical solution[14] are also presented for comparison. The result shows that Sandhu's scheme entails errors whenever there is a change of time step size. This phenomenon is particularly evident at $t = 1.1$ when the time step is increased from 0.1 to 10.

The solution for the excess pore pressure at $Z/H = 2/70$, obtained by both the present scheme and Sandhu's scheme deviate from the analytical solution greatly at the initial state up to the time $t = 0.2$ sec. This initial discrepancy decreases at the depth $Z/H = 4/70$. The reason can be explained as follows: At the time right after the load is applied, the pressure field at the surface jumps to equilibriate the applied pressure and drops sharply away from it. Under this situation, the linear interpolation function is inadequate to represent the pore pressure field at the vicinity of the load. This effect will be studied in details by mesh refinement in the following example.

Table 2. One dimensional consolidation problem. Comparison of the surface settlements in the irregular mesh modelled by the Q84 and Q94 elements

Time Factor $T_v = C_v t/H^2$ \ Element Type	Present Scheme		Analytical Solution
	Q84	Q94	
0.0	0.006290	0.007157	0.0
0.000021	0.007816	0.008437	0.0051669
0.000042	0.009109	0.009734	0.0073110
0.000105	0.012540	0.013018	0.0115600
0.000630	0.028890	0.028968	0.0283310
0.001154	0.038890	0.038868	0.0383400
0.022146	0.169307	0.169306	0.1671920
0.043137	0.236040	0.236040	0.2345820
0.064128	0.287470	0.287472	0.2857450
0.106111	0.369770	0.369765	0.3675680
0.316023	0.632350	0.631888	0.6282590
0.525936	0.782700	0.782697	0.7785830
1.155674	0.955180	0.955180	0.9531840
5.353924	0.999918	0.999918	0.9999980

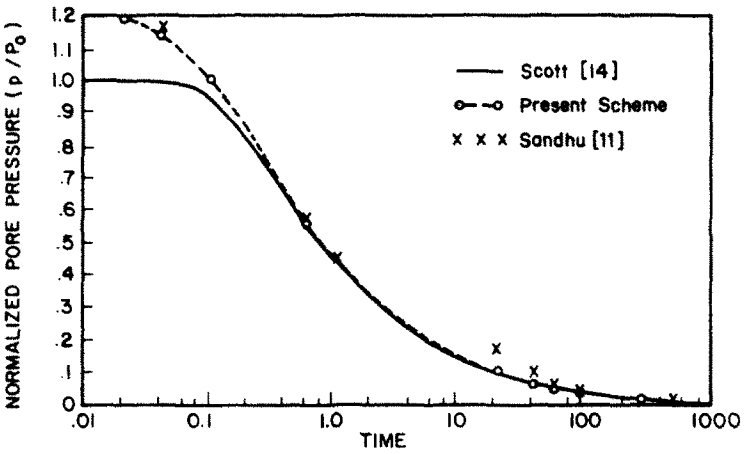

(a) EXCESS PORE PRESSURE HISTORY AT Z/H = 2/70

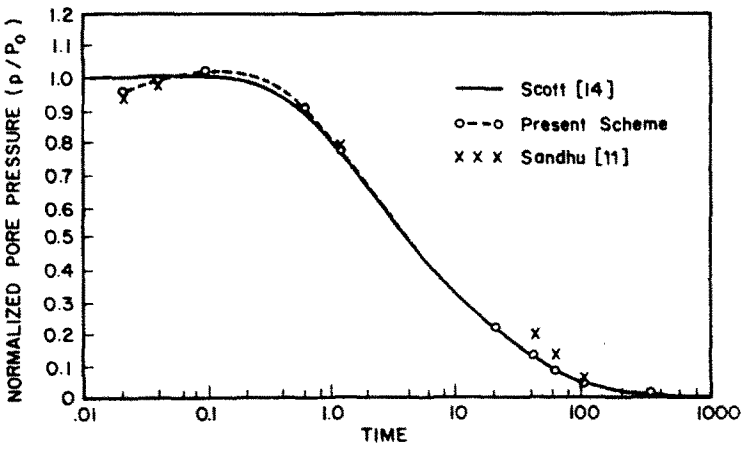

(b) EXCESS PORE PRESSURE HISTORY AT Z/H = 4/70

Fig. 5. Soil column consolidation problem; pore pressure history.

Plane strain consolidation problem

A linear elastic half space is subjected to a uniform strip load P_0. Three finite element meshes of Q84 elements are used, as shown in Fig. 6. The load is applied at time $t = 0$ and remains constant.

The vertical profile along the center line of the excess pore pressure at time $t = 0$ is given in Fig. 7(a). Errors are noticeable at the first element layer near the load in both the coarse and the first refined meshes. Since the size of the element next to the loaded surface is too coarse in both cases, the linear interpolation function adopted cannot adequately represent the large variation in pore pressure at the vicinity of the load. In the third mesh (Fig. 6c), the refinement is made so that a larger number of elements are concentrated at the load region. Almost the same amount of error remains in the first layer of elements; however, its position is now shifted upwards. Errors in pore pressure are also observed (Figs. 7a, b) at the half-space model boundaries. This is anticipated because a finite region is used to model the semi-infinite half space.

The excess pore pressure history at a point, $x_2/a = 0.5$ and $x_1/a = 0.0$, is presented in Fig. 8. An excellent overall solution is obtained with fine mesh 2(Fig. 5c). Sandhu's results and the analytical results[2] are also plotted for comparison. Both the fine mesh 1 (Fig. 6b) and Sandhu's scheme are not capable of giving correct pore pressure solutions in the earlier time stage due to the same reason mentioned.

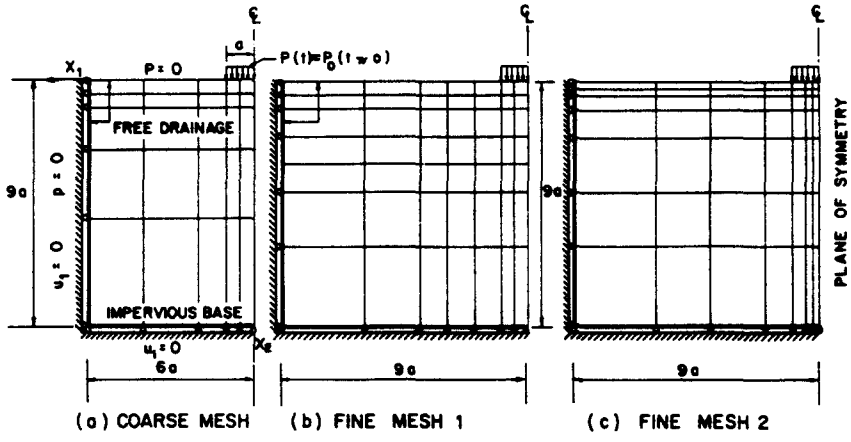

Fig. 6. Three finite element models for an elastic half space.

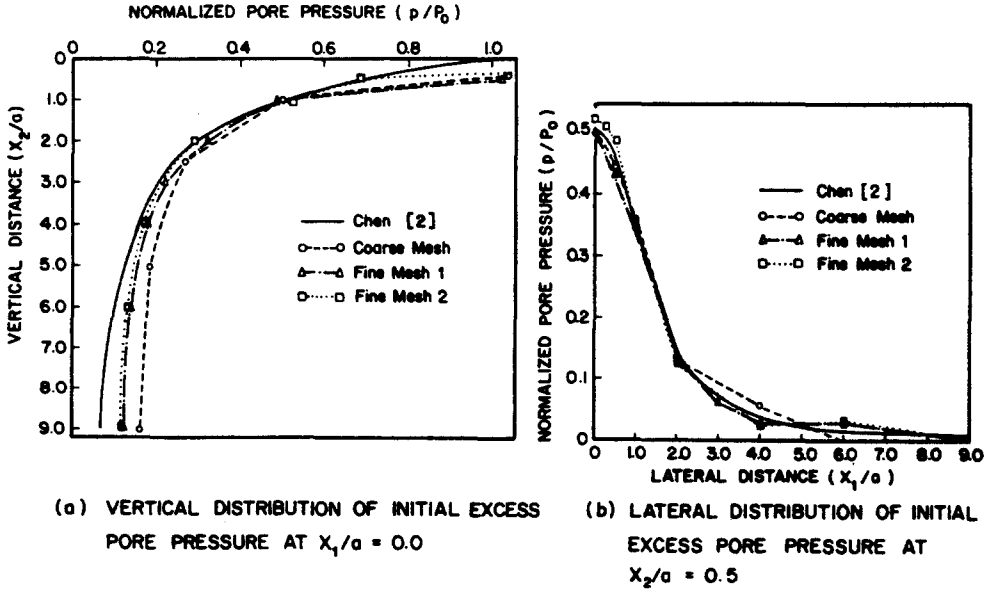

Fig. 7. Distribution of initial pore pressure in the elastic half space due to uniform strip load.

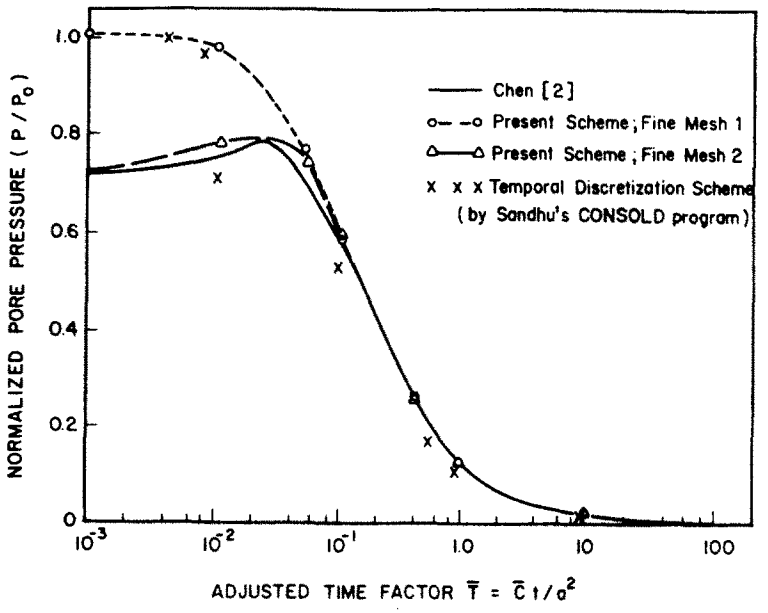

Fig. 8. Plane-strain consolidation problem; excess pore pressure history at $x_2/a = 0.5$, $x_1/a = 0.0$.

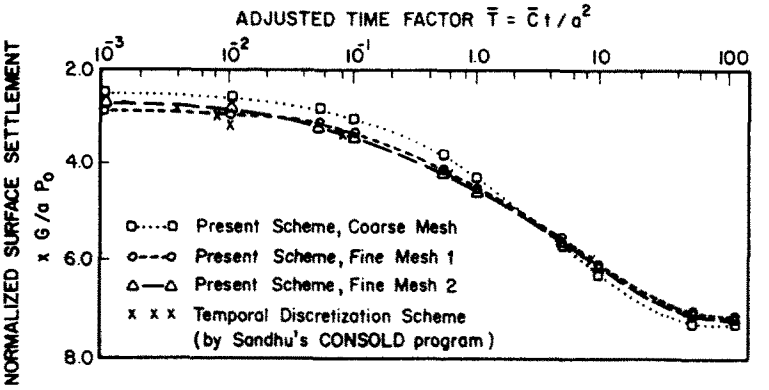

Fig. 9. Surface settlement of the half space due to consolidation.

Solution of the settlement at the center of the loaded surface, are plotted in Fig. 9 together with Sandhu's solution. Good agreement is seen between the two solutions.

Regarding computational efficiency, the CPU times required to solve this problem by the three meshes are compared in Table 3 with the time used by Sandhu's scheme. The present solutions are computed by the FEAP program[15] modified for this purpose. For relevant comparison, the problem is solved on the IBM 370/145 at the Regional Computer Center of Asian Institute of Technology, using the CONSOLD computer program developed by Sandhu, with $\Delta t = 0.0001$ over $[0, 0.0001]$, $\Delta t = 0.001$ over $[0.0001, 0.0101]$, $\Delta t = 0.01$ over $[0.0101, 0.1101]$, $\Delta t = 0.1$ over $[0.1101, 1.1101]$, and $\Delta t = 1.0$ over $[1.1101, 11.1101]$. The comparison shows that for the same finite element mesh, Sandhu's scheme needs about 8 times as much computer time as required by the present scheme.

Semi-infinite layer subjected to a strip load

A semi-infinite layer on an impervious base is subjected to a strip load. This semi-infinite layer is modelled by Q84 element mesh (Fig. 10) with the vertical boundary extended to a distance of 4(a) from the centre. Figure 10 shows the settlement at the center of the loaded surface. The exact solution by Gibson *et al.*[16] is also given for comparison; only small discrepancies are observed.

Table 3. Plane-strain consolidation problem. Computer time comparison between the present scheme and Sandhu's scheme[11] in IBM 370/145 CPU sec

Present Scheme with Q84			Sandhu's Scheme
Course Mesh (Fig. 6a)	Fine Mesh I (Fig. 6b)	Fine Mesh II (Fig. 6c)	Fine Mesh I (Fig. 6b)
125.91	629.90	632.0	5136.25

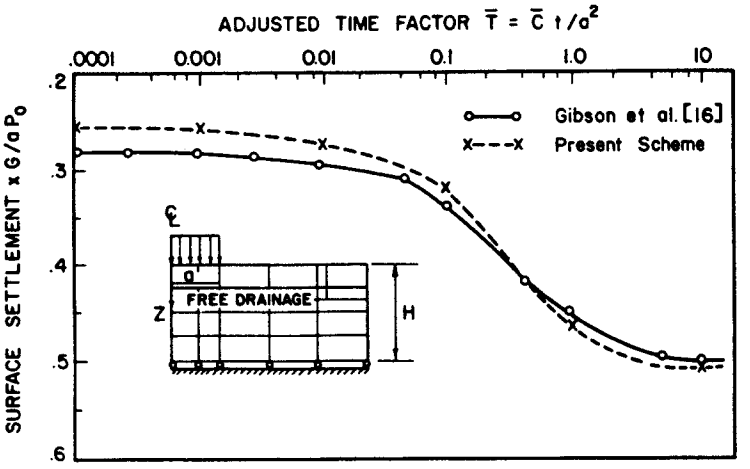

Fig. 10. Consolidation of a semi-infinite soil layer; surface settlement at the center.

CONCLUSIONS

In this study, the Q84 element is shown to be a reliable basis for the analysis of 2D linear elastic porous media. The combination of finite element idealization (in space) and the Laplace transform (of time variables) proves to be effective.

The present scheme gives better overall performance than time integration schemes. More notably, this superiority can be obtained with much less computational effort, since the solution for a specified time can be computed directly without a step-by-step marching. Higher reliability is anticipated because the present scheme is free of numerical instability.

REFERENCES

1. K. Terzaghi, *Theoretical Soil Mechanics*. Wiley, New York (1963).
2. R. L. Schiffman, T. F. Chen and J. C. Jordan, An analysis of consolidation theories. *J. Soil Mech. Foundation Div. ASCE* SM1 285–312 (1969).
3. M. A. Biot, General theory of three dimensional consolidation. *J. Appl. Phys.* 12, 155–164 (1941).
4. I. K. Lee, *Soil Mechanics—New Horizons*. Butterworths, London (1973).
5. R. S. Sandhu and E. L. Wilson, Finite element analysis of seepage in elastic media. *J. Engng Mech. Div. ASCE* 95(EM3), 641–652 (1969).
6. C. T. Hwang, N. R. Morgenstern and D. W. Murray, On solution of plane strain consolidation problems by finite element methods. *J. Can. Geotech.* 8, 109–118 (1971).
7. S. Valliappan, I. K. Lee and P. Boon Lualohr, Finite element analyses of consolidation problems. *Finite Element Methods in Flow Problems*, (Edited by J. T. Oden *et al.*). University of Albama at Huntsville Press, Alabama (1974).
8. Y. Yokoo, K. Yamagate and H. Nagaonka, Finite element method applied to Biot's consolidation theory. *Soils and Foundations* (Japanese Society of Soil Mechanics and Foundation Engineering) 11(1), 29–46 (1971).
9. Y. Yokoo, K. Yamagata and H. Nagaonka, Finite element analysis of consolidation following undrained deformation. *Soils and Foundations*, (Japanese Society of Soil Mechanics and Foundation Engineering) 11(4), 37–58 (1971).
10. G. Krause, Finite element schemes for porous elastic media. *J. Engng Mech. Div. ASCE* 104(EM3), 605–620 (1978).
11. R. S. Sandhu, H. Liu and K. J. Singh, Numerical performance of some finite element schemes for analysis of seepage in porous elastic media. *Int. J. Numer. Anal. Methods Geomech.* 1, 177–194 (1977).
12. P. Lancaster, *Lambda—Matrices and Vibrating Systems*. Pergamon Press, Oxford (1966).
13. B. Van der Pol and H. Bremmer, *Operational Calculus Based on the Two Sided Laplace Transform*. Cambridge University Press (1964).
14. R. F. Scott, *Principles of Soil Mechanics*. Addison Wesley, Reading, Mass. (1963).
15. O. C. Zienkiewicz, *The Finite Element Methods*, 3rd Edn, McGraw Hill, London (1977).
16. R. E. Gibson, R. L. Schipman and S. L. Pu, Plane strain and axially symmetric consolidation of a clay layer on a smooth impervious base. *Quart. J. Mech. Appl. Math.* 23(4), 505 (1970).